Energy Extraction from Rotating Black Hole in Effective Quantum Gravity via Comisso-Asenjo Magnetic Reconnection Process

Bing-Bing Chen (陈兵兵)[1] De-You Chen (陈德友)[2†] Zi-Chao Lin (林子超)[3] Jin-Tao Yao (姚金涛)[3]
Hao Yu (喻豪)[3] Xiao-Xiong Zeng (曾晓雄)[4]

[1]School of Mathematics, Physics and Statistics, Sichuan Minzu College, Ganzi 626100, China
[2]School of Science, Xihua University, Chengdu 610039, China
[3]Department of Physics and Chongqing Key Laboratory for Strongly Coupled Physics, Chongqing University, Chongqing 401331, China
[4]College of Physics and Electronic Engineering, Chongqing Normal University, Chongqing 401331, China

Abstract: We investigate energy extraction from a rotating quantum-corrected black hole in effective quantum gravity via the Comisso–Asenjo magnetic reconnection mechanism. We determine the allowed parameter space for energy extraction and evaluate the extraction efficiency for both circular and combined plasma streamlines. For circular streamlines, increasing the quantum parameter generally reduces the allowed parameter space. For combined streamlines, the plunging phase significantly expands the accessible radial range and broadens the extraction domain, while the relative influence of quantum corrections diminishes. Our results indicate the existence of a critical quantum parameter above which energy extraction ceases. In contrast to circular streamlines, the allowed parameter space for combined streamlines exhibits asymmetry with respect to the orientation angle, suggesting a preference for positive values of the optimal angle. We show that the quantum correction enhances the overall extraction efficiency and reduces the optimal reconnection radius. These results suggest that magnetic-reconnection-driven energy extraction may serve as a probe of effective quantum gravity effects in rotating black hole spacetime.

Keywords: Energy Extraction, Comisso-Asenjo mechanism, Quantum corrected black hole

DOI: 10.1088/1674-1137/aeb3ee **CSTR:**

CPC Accepted

I. INTRODUCTION

The magnetic reconnection process plays an important role in astrophysical phenomena [1−7]. In the recently proposed Comisso-Asenjo mechanism [8], this process is expected to be triggered by the plasmoid instability when antiparallel magnetic field lines undergo reversal [9−13]. It provides a spontaneous generation of plasma outflows within a highly magnetized plasma in the ergosphere and is a candidate source of the observed flare around the supermassive black hole Sagittarius A* [14−18]. Thus, the observational signatures of the magnetic reconnection process offer a new approach to testing new physics in the high-curvature regime. Energy extraction from black holes is one astrophysical scenario that can encode signatures of new physics. Classical examples include the Penrose process and the Blandford-Znajek mechanism [19−23], in which the outgoing particle generated through particle fission around a rotating black hole carries additional positive energy to infinity. However, the absence of an initiation mechanism and the low production rate of such particles make this process difficult to realize [24, 25]. In contrast, if the released magnetic energy is sufficiently strong, fast magnetic reconnection is believed to launch outflows with negative energy, providing a more feasible mechanism for extracting energy from the black hole [12, 13, 20, 26−50].

In effective theories with a classical spacetime structure, quantum corrections to energy extraction usually remain small. Generalizing spacetime to a nonclassical structure is expected to magnify these corrections [51, 52]. However, such a generalization usually requires an extension of the covariance principle in quantum spacetime [53], in which case formulating the dynamics at the kinematical quantum level becomes more challenging [54−63]. This is a long-debated issue in the symmetry-reduced effective theory of loop quantum gravity [64−71]. A straightforward approach to addressing it is to introduce a matter field to fix the diffeomorphism gauge [60, 61, 69, 71−73], while leaving the effective Hamiltonian constraint gauge-dependent. Recent proposals have pointed out that the reliance on gauge fixing by the matter field could be relaxed by imposing general covariance conditions [74, 75]. Effective Hamiltonian constraint candidates and a quantum-modified black hole solution can

Received 30 July 2026; Accepted 13 October 2026

† E-mail: deyouchen@hotmail.com

©2026 Chinese Physical Society and the Institute of High Energy Physics of the Chinese Academy of Sciences and the Institute of Modern Physics of the Chinese Academy of Sciences and IOP Publishing Ltd. All rights, including for text and data mining, AI training, and similar technologies, are reserved.

then be identified. In this paper, we discuss the nontrivial effect on the Comisso-Asenjo magnetic reconnection process in this covariant black hole model. We show that energy extraction can serve as a probe of the nontrivial effect of quantum corrections with a nonclassical spacetime structure.

This paper is organized as follows. In Section II, we introduce the rotating black hole in effective quantum gravity and analyze the geodesic motion. Section III is dedicated to the analysis of energy extraction via the Comisso-Asenjo magnetic reconnection mechanism, detailing the extraction parameter space and extraction efficiency. Finally, we present our conclusions in Section IV.

II. ROTATING QUANTUM CORRECTED BLACK HOLES

We begin with the covariant black hole model proposed in Ref. [74], whose line element in a static, spherically symmetric spacetime is given by

$$ds^2 = -f(r)dt^2 + \frac{dr^2}{f(r)} + r^2\left(d\theta^2 + \sin^2\theta d\phi^2\right), \tag{1}$$

the metric function read as

$$\begin{aligned} f(r) &= 1 - \frac{2M}{r} + \frac{\zeta^2}{r^2}\left(1 - \frac{2M}{r}\right)^2 \\ &= \frac{(r-r_+)(r-r_-)\left(r^2 + r_-r + r_-^2 + \zeta^2\right)}{r^4}, \end{aligned} \tag{2}$$

where

$$r_- = \frac{3^{1/3}\left[\zeta^2\left(9M + \sqrt{3}\sqrt{27M^2 + \zeta^2}\right)\right]^{2/3} - 3^{2/3}\zeta^2}{3\left[\zeta^2\left(9M + \sqrt{3}\sqrt{27M^2 + \zeta^2}\right)\right]^{1/3}}, \tag{3}$$

$$r_+ = 2M. \tag{4}$$

Here, M denotes the ADM mass, while ζ is a non-negative quantum correction parameter proportional to the Planck length [74]. This static, spherically symmetric solution has an inner horizon at $r = r_-$ and an outer horizon at $r = r_+$. It reduces to the Schwarzschild solution in the limit $\zeta \to 0$. The corresponding rotating geometry can be generated using the modified Newman–Janis algorithm [76], in which the Eddington–Finkelstein coordinate transformation provides a method for defining the rotation parameter a. A pull-back transformation to Boyer–Lindquist coordinates then converts the seed metric into [77]

$$\begin{aligned} ds^2 = &-\frac{\Delta - a^2\sin^2\theta}{\Sigma}dt^2 + \frac{\Sigma}{\Delta}dr^2 + \Sigma d\theta^2 \\ &+ \frac{\sin^2\theta}{\Sigma}\left[\left(r^2 + a^2\right)^2 - a^2\Delta\sin^2\theta\right]d\varphi^2 \\ &- \frac{2a\sin^2\theta}{\Sigma}\left(r^2 + a^2 - \Delta\right)dtd\varphi, \end{aligned} \tag{5}$$

with

$$\Sigma = r^2 + a^2\cos^2\theta, \tag{6a}$$

$$\Delta = r^2 - 2Mr + a^2 + \zeta^2\left(1 - \frac{2M}{r}\right)^2. \tag{6b}$$

In the classical limit $\zeta \to 0$, this metric reduces to the Kerr spacetime.

The horizon of this rotating quantum-corrected black hole is determined by the root of $g^{rr} = 0$, which corresponds to

$$\Delta = \frac{(r-r_+)(r-r_-)\left(r^2 + r_-r + r_-^2 + \zeta^2\right)}{r^2} + a^2 = 0. \tag{7}$$

This equation admits inner and outer event horizons, whose radii satisfy $r_- \leqslant r_{\rm C} \leqslant r_{\rm H} \leqslant r_+$. Figure 1 displays the horizon structure in the $(a/M, \zeta)$ parameter space. In the limit $a \to 0$, the parameter ζ decouples from the radius of the outer horizon and is therefore not bounded from above. For a spinning black hole, the inner horizon radius $r_{\rm C}$ increases with the quantum correction parameter ζ and the spin a, whereas the event horizon radius $r_{\rm H}$ exhibits the opposite behavior. There exists a set of critical parameter values at which the two horizons coincide and the black hole becomes extremal. Below this threshold, the spacetime contains two distinct horizons, whereas above it, a naked singularity is present. Furthermore, by evaluating the area of the event horizon, one can determine the irreducible mass $M_{\rm irr}$ of the black hole. As shown in Figure 2, for a fixed spin a (or ζ), the irreducible mass decreases monotonically as ζ (or a) increases. This behavior indicates that increasing these parameters can enhance the extractable rotational energy of the black hole. In contrast, in the extremal configuration, where the inner and event horizons coincide, $M_{\rm irr}$ increases with ζ, implying that the quantum correction reduces the total extractable energy of the extremal black hole.

Following Ref. [8], we assume that magnetic reconnection occurs in the equatorial plane. Energy extraction takes place in the ergoregion, that is, the region between the outer event horizon and the outer infinite-redshift surface. In the equatorial plane, the radius of the latter can be derived from the condition $g_{tt} = 0$. As with the event hori-

CPC Accepted

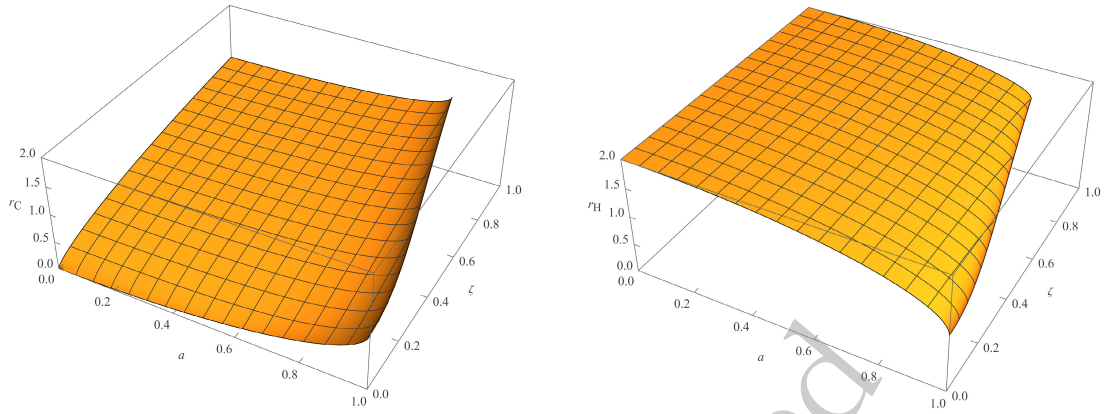

Fig. 1. The inner-horizon radius $r_{\rm C}$ (left panel) and the event-horizon radius $r_{\rm H}$ (right panel) as functions of the quantum parameter ζ and the black-hole spin a.

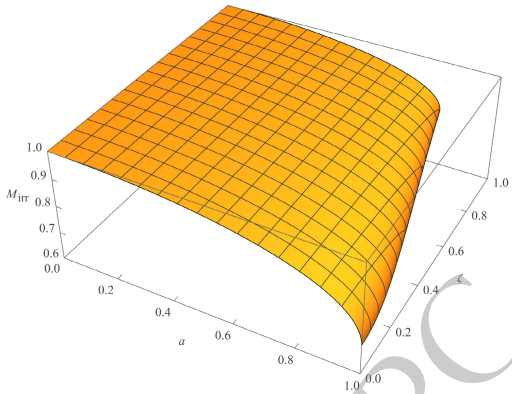

Fig. 2.

zon, the outer and inner infinite-redshift surfaces are located at r_+ and r_-, respectively. For geodesic motion in the rotating quantum-corrected spacetime, there are three conserved quantities: the energy E, the z-component of angular momentum L, and the Carter constant Q. In the present work, we focus on geodesic motion confined to the equatorial plane, with $\theta \equiv \pi/2$ and $\frac{d\theta}{d\tau} = 0$. Consequently, the Carter constant vanishes, $Q = 0$, and the polar component of the four-velocity is identically zero. Using the Hamilton-Jacobi equation [78], the first-order geodesic equations in the equatorial plane can be written as

$$\Sigma U^t = \frac{(r^2+a^2)\left[(r^2+a^2)E - aL\right]}{\Delta} - a(aE-L), \tag{8a}$$

$$\Sigma U^r = \pm\sqrt{R(r)}, \tag{8b}$$

$$\Sigma U^\theta = 0, \tag{8c}$$

$$\Sigma U^\varphi = \frac{a\left[(r^2+a^2)E - aL\right]}{\Delta} - (aE-L), \tag{8d}$$

where

$$R(r) = \left[\left(r^2+a^2\right)E - aL\right]^2 - \Delta\left[(aE-L)^2 + m^2 r^2\right]. \tag{9}$$

Here, $m^2 = 1$ corresponds to timelike geodesics, whereas $m^2 = 0$ corresponds to null geodesics. From the definition of $R(r)$, the radius of the photon sphere is determined by

$$R(r_{\rm PH}) = 0 \qquad \text{and} \qquad R'(r_{\rm PH}) = 0, \tag{10}$$

where the prime denotes differentiation with respect to r. Similarly, the radius of the innermost stable circular orbit (ISCO) can be obtained from

$$R(r_{\rm ISCO}) = 0, \qquad R'(r_{\rm ISCO}) = 0, \qquad R''(r_{\rm ISCO}) = 0. \tag{11}$$

Fig. 3 shows the dependence of the photon sphere radius and the ISCO radius on the quantum parameter ζ. The effect of ζ is relatively weak in the low-spin regime but becomes significant as the black hole acquires greater angular momentum. In particular, a larger value of ζ shifts the photon sphere inward and reduces the critical spin, as indicated by the earlier termination of the curves. The ISCO radius exhibits similar behavior.

III. ENERGY EXTRACTION VIA COMISSO-ASENJO PROCESS

A. Comisso–Asenjo Process

In this subsection, we briefly summarize the basic framework for energy extraction via the Comisso–Asenjo magnetic reconnection mechanism. Because this process

CPC Accepted

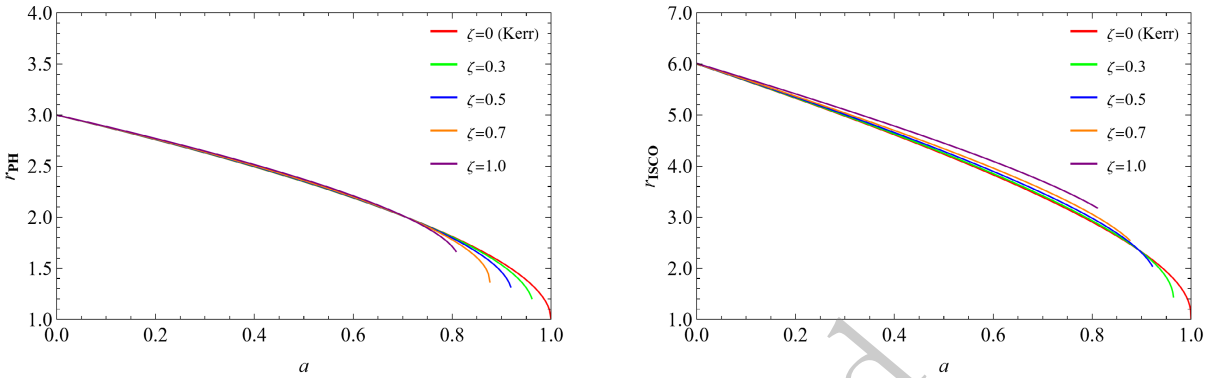

Fig. 3. Photon-sphere radius (left panel) and ISCO radius (right panel) as functions of the black hole spin a for several values of the quantum parameter ζ.

occurs in a stationary and axisymmetric spacetime, it is convenient to formulate the plasma dynamics in the zero-angular-momentum-observer (ZAMO) frame [24, 28, 79]. In this frame, the spacetime is locally Minkowskian, which simplifies the analysis of the plasma's kinematic and energetic properties. The line element can be written as follows:

$$ds^2 = -\alpha^2 dt^2 + \sum_{i=1}^{3}(\sqrt{g_{ii}}dx^i - \alpha\beta^i dt)^2, \tag{12}$$

where α is the lapse function, and $\beta^i = \sqrt{g_{ii}}\omega^i/\alpha$ is the shift vector associated with frame dragging. Explicitly, we have

$$\alpha = \sqrt{\frac{g_{t\varphi}^2}{g_{\varphi\varphi}} - g_{tt}}, \qquad \beta^i = (0,0,\beta^\varphi), \qquad \omega^i = \left(0,0,-\frac{g_{t\varphi}}{g_{\varphi\varphi}}\right). \tag{13}$$

Using the orthonormal tetrad of the ZAMOs, we introduce the rest frame of the bulk plasma as [28, 79]

$$e^\mu_{[0]} = \hat{\gamma}_s\left[\hat{e}^\mu_{(t)} + \hat{v}_s^{(r)}\hat{e}^\mu_{(r)} + \hat{v}_s^{(\varphi)}\hat{e}^\mu_{(\varphi)}\right], \tag{14a}$$

$$e^\mu_{[1]} = \frac{1}{\hat{v}_s}\left[\hat{v}_s^{(\varphi)}\hat{e}^\mu_{(r)} - \hat{v}_s^{(r)}\hat{e}^\mu_{(\varphi)}\right], \qquad e^\mu_{[2]} = \hat{e}^\mu_{(\theta)}, \tag{14b}$$

$$e^\mu_{[3]} = \hat{\gamma}_s\left[\hat{v}_s\hat{e}^\mu_{(t)} + \frac{\hat{v}_s^{(r)}}{\hat{v}_s}\hat{e}^\mu_{(r)} + \frac{\hat{v}_s^{(\varphi)}}{\hat{v}_s}\hat{e}^\mu_{(\varphi)}\right], \tag{14c}$$

where $\hat{v}_s^2 = \hat{v}_s^{(r),2} + \hat{v}_s^{(\varphi),2}$ denotes the squared magnitude of the plasma three-velocity measured in the ZAMO frame, and $\hat{\gamma}_s$ denotes the corresponding Lorentz factor. We assume that the bulk plasma follows geodesic motion. Its four-velocity U^μ can then be projected onto the ZAMO tetrad as follows:

$$U^\nu\hat{e}^{(\mu)}_\nu = \hat{\gamma}_s\{1,\hat{v}_s^{(r)},0,\hat{v}_s^{(\varphi)}\} = \left\{\frac{E-\omega^\varphi L}{\alpha}, U^r\sqrt{g_{rr}}, 0, \frac{L}{\sqrt{g_{\varphi\varphi}}}\right\}, \tag{15}$$

where E and L are the conserved energy and angular momentum of the plasma motion, respectively. Following Refs. [28, 79], we consider two representative types of bulk plasma streamlines. In the circular-streamline case, the radial velocity vanishes, $\hat{v}_s^{(r)} = 0$. Thus, the plasma follows a circular orbit, with radii extending down to the critical radius determined by the photon sphere. In the combined-streamline case, the plasma initially undergoes circular motion outside the ISCO and then plunges inward after crossing it.

Near the equatorial current sheet, the local configuration of antiparallel magnetic field lines is unstable to the plasmoid instability. Therefore, small perturbations can trigger fast magnetic reconnection and produce a pair of plasmoids ejected in opposite directions. Their four-velocities are taken to be

$$u^\mu_\pm = \gamma_{\rm out}\left[e^\mu_{[0],0} \pm v_{\rm out}\left(e^\mu_{[3],0}\cos\xi + e^\mu_{[1],0}\sin\xi\right)\right], \tag{16}$$

where the symbols "+" and "−" denote the two plasmoids ejected in opposite directions. Here, we adopt the standard model of fast reconnection, in which the outflow speed is given by $v^2_{\rm out} = \frac{\sigma}{1+\sigma}$, where σ is the local magnetization at the reconnection point and $\gamma_{\rm out}$ is the associated Lorentz factor. The orientation angle ξ is treated as a free parameter in the interval $(-\pi/2,\pi/2)$ [79]. The energy-extraction efficiency is defined as [8]

$$\eta = \frac{e^\infty_+}{e^\infty_+ + e^\infty_-}, \tag{17}$$

where $e^\infty_\pm$ denote the energy at infinity per unit enthalpy

CPC Accepted

carried by the two plasmoids. In the present setup, these quantities are given by [8, 28]

$$e^{\infty}_{\pm} = \alpha\hat{\gamma}_s\gamma_{\rm out}\left[1+\beta^{\varphi}\hat{v}^{(\varphi)}_s \pm v_{\rm out}\left(\hat{v}_s + \beta^{\varphi}\frac{\hat{v}^{(\varphi)}_s}{\hat{v}_s}\right)\cos\xi \mp v_{\rm out}\beta^{\varphi}\frac{\hat{v}^{(r)}_s}{\hat{\gamma}_s\hat{v}_s}\sin\xi\right] - \frac{\alpha}{4\hat{\gamma}_s\gamma_{\rm out}(1\pm\hat{v}_s v_{\rm out}\cos\xi)}. \tag{18}$$

This expression is obtained under the assumption that the magnetic energy released by reconnection is converted into the kinetic energy of the plasmoids with sufficiently high efficiency, such that the hydrodynamic contribution dominates the energy budget at infinity. Energy extraction becomes possible when one plasmoid falls into the black hole with negative energy at infinity, while the other escapes to infinity with positive energy [8, 38]; namely,

$$e^{\infty}_{-} < 0 \qquad \text{and} \qquad e^{\infty}_{+} > 0. \tag{19}$$

Under this condition, the energy carried by the outgoing plasmoid exceeds the locally supplied energy. This provides a mechanism for extracting rotational energy from the black hole.

B. Parameter space for Energy Extraction

The hydrodynamic energy at infinity per unit plasma enthalpy depends on the black hole mass M, the spin a, the radial position r_X of the dominant magnetic reconnection point (the X point), the plasma magnetization σ, the orientation angle ξ, and the quantum correction parameter ζ. In the following, we work in units with $M=1$, so that a, r, and ζ are measured in units of M.

Figure 4 illustrates the parameter space for energy extraction via the Comisso-Asenjo magnetic reconnection mechanism. Specifically, the panels are generated with $\sigma = 100$ and $\xi = \pi/12$ to characterize the plasma environment and field geometry relevant to the reconnection process. The top-left panel shows the parameter space of circular streamlines in the $a - r_X$ plane for several representative values of the quantum parameter ζ. The shift of the parameter space with respect to ζ indicates that the quantum correction can modify the condition for efficient magnetic reconnection energy extraction. In general, increasing the quantum parameter ζ reduces the parameter space for energy extraction. For near-extremal black holes, the reconnection mechanism remains effective, and energy can always be extracted. The right boundary is related to the critical spin of the extremal black hole, which is affected by the parameter ζ. The shift of this boundary therefore indicates a significant contribution from the quantum deformation. In contrast, the deformation has only a weak impact on the minimum spin threshold for energy extraction. As ζ continues to increase, the corresponding extraction region gradually departs from that of the Kerr spacetime, eventually leading to a region that no longer overlaps with the Kerr case. This behavior also appears in the bottom-left panel. For the case of $a = 0.84$, the parameter space for energy extraction is already separated from those associated with higher spins, indicating that sufficiently large quantum deformation can significantly modify the parameter space compared with the Kerr case. Furthermore, there exists a critical value of the quantum parameter ζ above which energy extraction via magnetic reconnection becomes impossible. For the parameter configuration adopted in Figure 4, this critical value is approximately 0.92.

In the right panels of Figure 4, we show the parameter space for energy extraction for combined streamlines. For this class of streamlines, the radial range of the energy extraction region becomes noticeably broader than that for circular streamlines. This broadening occurs because combined streamlines can eventually plunge into the black hole. During this phase, additional fragmentation of the flow occurs, allowing part of the plasma to be expelled outward and carry away extra energy. Consequently, the effective reconnection-driven energy extraction process has a significantly wider radial range. In the $a - r_X$ plane, the right boundary behaves similarly to that in the previous case. However, the left boundary becomes insensitive to the quantum parameter, indicating a robust minimum spin threshold close to $a \approx 0.28$. As a result, the energy-extraction region is not completely separated from that of the Kerr case. The quantum parameter also has a critical value for this type of streamline. With the parameter configuration adopted in Figure 4, we find that this value is approximately 6.3, beyond which energy extraction no longer occurs.

In addition, previous studies [45, 79] have shown that the orientation angle ξ can make different contributions to energy extraction for the two types of streamlines. This feature can be checked straightforwardly using Eq. (18). The expression is invariant under the transformation $\xi \to -\xi$ for the circular streamline with $\hat{v}^{(r)}_s = 0$, whereas it is not invariant for the combined streamline because of the nonvanishing radial velocity component $\hat{v}^{(r)}_s \neq 0$. Following the analyses presented in Refs. [45, 79], one can introduce an optimal orientation angle that maximizes the efficiency of energy extraction in the high-magnetization limit. This angle is given by

$$\xi_{\rm max} = \arctan\frac{-\beta^{\varphi}\hat{v}^{(r)}_s}{\hat{\gamma}_s\hat{v}^2_s + \beta^{\varphi}\hat{\gamma}_s\hat{v}^{(\varphi)}_s}. \tag{20}$$

For circular plasma motion, in which the radial velocity

CPC Accepted

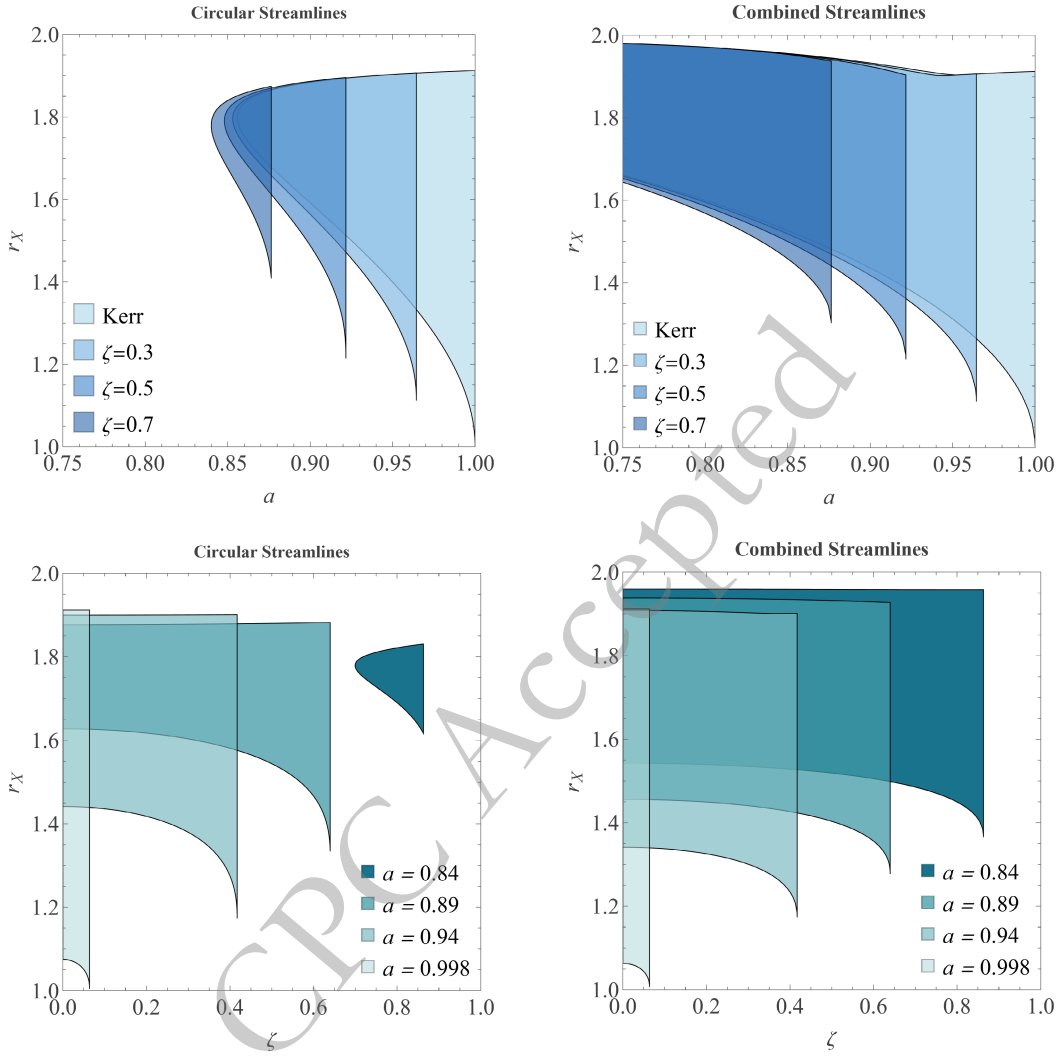

Fig. 4. Energy-extraction regions in the $a-r_X$ plane (upper panels) and $\zeta-r_X$ plane (lower panels) for circular streamlines (left panels) and combined streamlines (right panels). The upper panels show the results for $\zeta=\{0(\text{Kerr}),0.3,0.5,0.7\}$, whereas the lower panels show the results for black hole spins of $a=\{0.84,0.89,0.94,0.998\}$. The magnetization and orientation angle are set to $\sigma=100$ and $\xi=\pi/12$, respectively.

component is zero, this expression reduces to $\xi_{\max}=0$. By contrast, for plunging plasma flows with a nonzero radial component, the maximum orientation angle satisfies $\xi_{\max}>0$. In Figure 5, we present the parameter space for energy extraction in the $\xi-r_X$ plane for several values of the quantum parameter ζ. As ζ increases, the parameter space in the $\xi-r_X$ plane expands, with the lower boundary shifting toward smaller r_X. For circular streamlines (left panel), the parameter space is symmetric with respect to the axis $\xi=0$. In contrast, for combined streamlines (right panel), this symmetry is not preserved; instead, the parameter space exhibits a clear bias toward the $\xi>0$ side, reflecting the fact that the optimal orientation angle satisfies $\xi_{\max}>0$.

C. Efficiency for Energy Extraction

We now examine the efficiency of energy extraction from a rotating quantum-corrected black hole. During the energy-extraction process driven by magnetic reconnection, part of the black hole's rotational energy is transferred to the plasma, generating energetic outflows. Magnetic reconnection redistributes the angular momentum and energy of plasma particles, with a fraction of the particles attaining negative-energy states while others are accelerated outward. As a consequence, energy can be extracted from the black hole. To quantify the effectiveness of this mechanism, we introduce the energy-extraction efficiency defined in Eq. (17). The condition $e_-^\infty<0$ is necessary to initiate the extraction process. Once this process begins, part of the plasma falls into the black hole with negative energy, while the escaping component transports additional energy to infinity. Consequently, the extraction efficiency necessarily exceeds 1.

As shown in Figure 6, the overall efficiency first in-

CPC Accepted

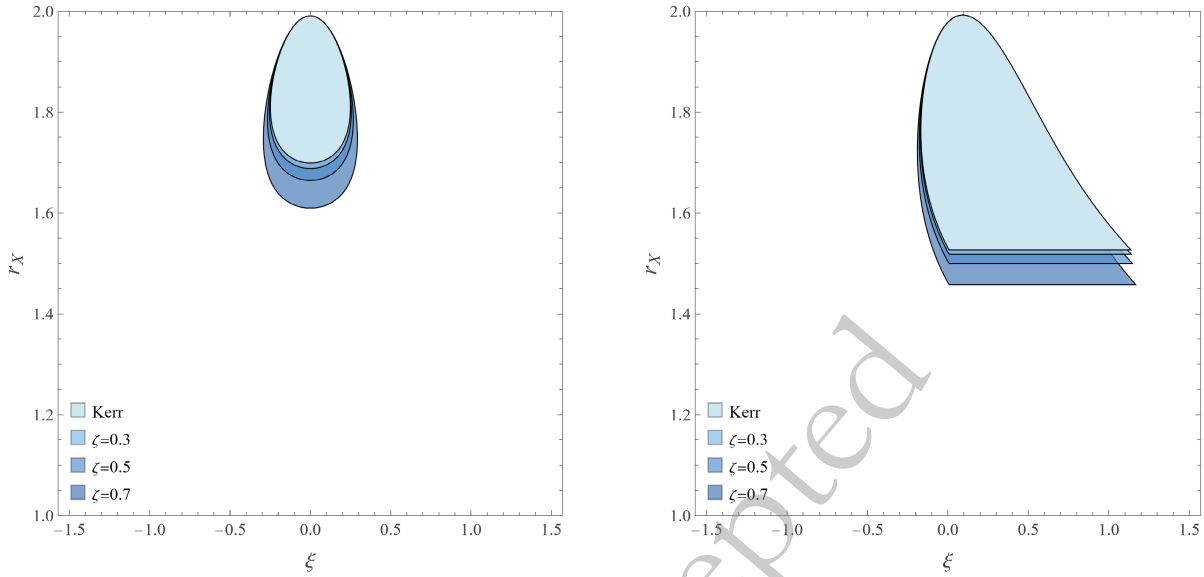

Fig. 5. Energy extraction region in the $\xi - r_X$ plane for circular streamlines (left panel) and combined streamlines (right panel). The black hole spin and magnetization are set to $a = 0.85$ and $\sigma = 100$, respectively.

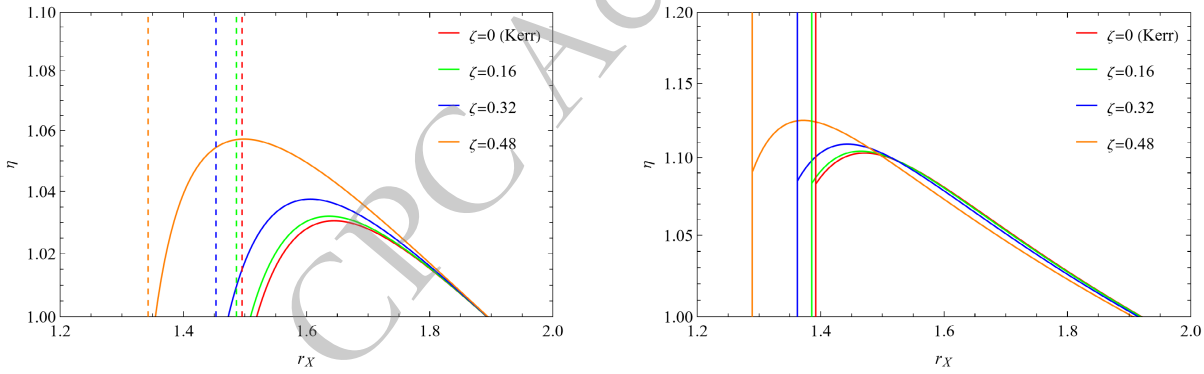

Fig. 6. Energy extraction efficiency η for circular streamlines (left panel) and combined streamlines (right panel). The vertical dashed lines denote the photon-sphere location, and the vertical solid lines indicate the event-horizon position. The black hole spin, magnetization, and orientation angle are set to $a = 0.92$, $\sigma = 100$, and $\xi = \pi/12$, respectively.

creases with the reconnection radius r_X, reaches a maximum, and then gradually decreases. This behavior reflects a competition between the rotational energy available to the plasma and the gravitational binding energy of the black hole. When the reconnection point is too close to the horizon, the strong gravitational potential suppresses the outward energy flux, thereby reducing the extraction efficiency. As r_X increases before the turning point, the plasma can extract rotational energy more effectively, and the efficiency increases. At radii beyond the maximum, however, the rotational energy available to the plasma gradually decreases, leading to a decline in the extraction efficiency. Figure 6 also shows that the quantum deformation increases the overall efficiency and reduces the optimal reconnection radius for both circular and combined streamlines. It is worth noting that, compared with circular streamlines, combined streamlines have a noticeably higher efficiency, with the peak occurring closer to the black hole. This is mainly because the plunging motion of the plasma allows the conversion of additional kinetic energy into outgoing energy during the fragmentation process.

IV. CONCLUSION

In this work, we investigated the extraction of rotational energy from a rotating quantum-corrected black hole within effective quantum gravity via the Comisso-Asenjo magnetic reconnection mechanism. We first analyzed the properties of the rotating spacetime, including the horizon structure, the irreducible mass, and the characteristic radii relevant to plasma motion on the equatorial plane. We found that the effects of the quantum correction are most pronounced in the high-spin regime, with the parameter ζ decreasing the outer horizon radius and

CPC Accepted

the maximum spin while increasing the inner horizon radius. We also found that the photon sphere and the ISCO exhibit similar behavior, indicating that the quantum correction can directly influence the admissible reconnection region for plasma motion.

We then studied the conditions for energy extraction and identified the corresponding parameter space for both circular and combined plasma streamlines. For circular streamlines, we found that the quantum correction shrinks the parameter space for energy extraction and eventually terminates the process when the parameter ζ reaches a critical value. For the representative parameter choice ($\sigma = 100$ and $\xi = \pi/12$) adopted in our analysis, we found this critical value to be $\zeta \sim 0.92$. In contrast, for combined streamlines, the plunging phase substantially expands the radial range, so the extraction region is much larger and allows a considerably higher critical value, $\zeta \sim 6.3$. We showed that the minimum spin threshold for the combined streamline case is weakly affected by the quantum correction and remains close to $a \approx 0.28$.

Another important difference between the two streamlines concerns the orientation angle. For circular streamlines, the radial plasma velocity vanishes, so the energy extraction condition is invariant under $\xi \to -\xi$. In contrast, the plunging phase of combined streamlines breaks this symmetry and therefore gives rise to a preferred positive optimal orientation angle, $\xi_{\max} > 0$. Correspondingly, the parameter space in the $\xi - r_X$ plane is symmetric for circular streamlines, whereas it becomes skewed toward positive ξ for combined streamlines.

Finally, we examined the efficiency of the magnetic-reconnection-driven extraction process. We used the condition that the efficiency exceeds 1 to indicate the onset of energy extraction. We found that, for both classes of streamlines, the efficiency first increases with the reconnection radius, reaches a maximum, and then gradually decreases. We further found that the quantum correction enhances the overall efficiency and decreases the optimal reconnection radius. Compared with circular streamlines, the combined streamline case extracts energy more efficiently, with the turning point closer to the event horizon. This behavior reflects the additional contribution from the plunging motion of the plasma.

Overall, our results indicate that quantum corrections can leave clear imprints on both the parameter space and the efficiency of magnetic-reconnection-driven energy extraction around a rotating black hole. In this sense, the Comisso-Asenjo process may provide a useful probe of effective quantum gravity effects in strong-field black hole environments. It would be interesting in future work to extend the present analysis to other quantum-corrected rotating black hole models and more realistic plasma environments, and to explore possible observational implications for high-energy black hole accretion systems.

CPC Accepted

References

[1] E. G. Zweibel and M. Yamada, Ann. Rev. Astron. Astrophys. **47**, 291 (2009)
[2] M. Yamada, R. Kulsrud, and H. Ji, Rev. Mod. Phys. **82**, 603 (2010)
[3] L. Sironi, D. A. Uzdensky, and D. Giannios, Ann. Rev. Astron. Astrophys. **63**, 127 (2025)
[4] F. Yuan, J. Lin, K. Wu, and L. C. Ho, Mon. Not. Roy. Astron. Soc. **395**, 2183 (2009)
[5] H. Yang, F. Yuan, H. Li, Y. Mizuno, F. Guo, R. Lu, L. C. Ho, X. Lin, A. A. Zdziarski, and J. Wang, Sci. Adv. **10**, adn3544 (2024)
[6] L. Xi and Y. Feng, Mon. Not. Roy. Astron. Soc. **531**, 3136 (2024)
[7] A. Nathanail, Y. Mizuno, I. Contopoulos, C. M. Fromm, A. Cruz-Osorio, K. Moriyama, and L. Rezzolla, Astron. Astrophys. **693**, A56 (2025)
[8] L. Comisso and F. A. Asenjo, Phys. Rev. D **103**, 023014 (2021)
[9] N. F. Loureiro, A. A. Schekochihin, and S. C. Cowley, Phys. Plasmas **14**, 100703 (2007)
[10] D. A. Uzdensky, N. F. Loureiro, and A. A. Schekochihin, Phys. Rev. Lett. **105**, 235002 (2010)
[11] L. Sironi, D. Giannios, and M. Petropoulou, Mon. Not. Roy. Astron. Soc. **462**, 48 (2016)
[12] L. Comisso, M. Lingam, Y. M. Huang, and A. Bhattacharjee, Phys. Plasmas **23**, 100702 (2016)
[13] L. Comisso, M. Lingam, Y.-M. Huang, and A. Bhattacharjee, Astrophys. J. **850**, 142 (2017)
[14] K. Akiyama *et al*. (Event Horizon Telescope), Astrophys. J. Lett. **930**, L12 (2022)
[15] T. Do, G. Witzel, A. K. Gautam, Z. Chen, A. M. Ghez, M. R. Morris, E. E. Becklin, A. Ciurlo, M. Hosek, G. D. Martinez, K. Matthews, S. Sakai, and R. Schödel, Astrophys. J. Lett. **882**, L27 (2019)
[16] B. Ripperda, F. Bacchini, and A. Philippov, Astrophys. J. **900**, 100 (2020)
[17] N. Aimar, A. Dmytriiev, F. H. Vincent, I. E. Mellah, T. Paumard, G. Perrin, and A. Zech, Astron. Astrophys. **672**, A62 (2023)
[18] G. Sen, D. Maity, and S. Das, Phys. Rev. D **112**, 083047 (2025)
[19] R. Penrose, Riv. Nuovo Cim. **1**, 252 (1969)
[20] C. Meringolo, F. Camilloni, and L. Rezzolla, Astrophys. J. Lett. **992**, L8 (2025)
[21] I. Okamoto, Publ. Astron. Soc. Jap. **58**, 1047 (2006)
[22] R. D. Blandford and R. L. Znajek, Mon. Not. Roy. Astron. Soc. **179**, 433 (1977)
[23] J.-P. Lasota, E. Gourgoulhon, M. Abramowicz, A. Tchekhovskoy, and R. Narayan, Phys. Rev. D **89**, 024041 (2014)
[24] J. M. Bardeen, W. H. Press, and S. A. Teukolsky, Astrophys. J. **178**, 347 (1972)
[25] R. M. Wald, Astrophys. J. **191**, 231 (1974)
[26] M. Khodadi, Phys. Rev. D **105**, 023025 (2022)
[27] S.-W. Wei, H.-M. Wang, Y.-P. Zhang, and Y.-X. Liu, JCAP (04), 050 (2022)

[28] B. Chen, Y. Hou, J. Li, and Y. Shen, Phys. Rev. D **110**, 063003 (2024)
[29] W. Liu, Astrophys. J. **925**, 149 (2022)
[30] A. Carleo, G. Lambiase, and L. Mastrototaro, Eur. Phys. J. C **82**, 776 (2022)
[31] C.-H. Wang, C.-Q. Pang, and S.-W. Wei, Phys. Rev. D **106**, 124050 (2022)
[32] S. Shaymatov, M. Alloqulov, B. Ahmedov, and A. Wang, Phys. Rev. D **110**, 044005 (2024)
[33] S.-J. Zhang, JCAP (07), 042 (2024)
[34] X.-X. Zeng and K. Wang, Phys. Rev. D **112**, 064080 (2025)
[35] X.-X. Zeng and K. Wang, Phys. Rev. D **112**, 064032 (2025)
[36] F. Long, S. Wang, S. Chen, and J. Jing, Eur. Phys. J. C **85**, 26 (2025)
[37] J.-T. Yao, K.-J. He, Z.-C. Lin, and H. Yu, Phys. Lett. B **878**, 140562 (2026)
[38] Y. Shen and H.-Y. YuChih, Phys. Rev. D **111**, 023003 (2025)
[39] X. Ye, C.-H. Wang, and S.-W. Wei, JCAP (12), 030 (2023)
[40] S. Rodriguez, A. Sidler, L. Rodriguez, and L. R. Ram-Mohan, Phys. Dark Univ. **48**, 101961 (2025)
[41] K. Wang and X.-X. Zeng, JCAP (11), 026 (2025)
[42] J. A. Rueda and R. Ruffini, Eur. Phys. J. C **83**, 960 (2023)
[43] M. Khodadi, D. F. Mota, and A. Sheykhi, JCAP (10), 034 (2023)
[44] B. Zhao, C.-H. Wang, and S.-W. Wei, Chin. Phys. C **50**, 055102 (2026)
[45] H.-Y. YuChih and Y. Shen, Phys. Rev. D **112**, 104016 (2025)
[46] D. Ortiqboev, F. Javed, F. Atamurotov, A. Abdujabbarov, and G. Mustafa, Phys. Dark Univ. **46**, 101615 (2024)
[47] E. Battista, Phys. Rev. D **109**, 026004 (2024)
[48] Z. Li and F. Yuan, Phys. Rev. D **108**, 024039 (2023)
[49] Z.-Y. Fan, F. Zhou, Y. Li, M. Guo, and B. Chen, Phys. Rev. D **111**, 064067 (2025)
[50] Z.-Y. Fan, Y. Li, F. Zhou, and M. Guo, Phys. Rev. D **110**, 104044 (2024)
[51] M. Bojowald, G. Calcagni, and S. Tsujikawa, Phys. Rev. Lett. **107**, 211302 (2011)
[52] M. Bojowald, G. Calcagni, and S. Tsujikawa, JCAP (11), 046 (2011)
[53] I. H. Belfaqih, M. Bojowald, S. Brahma, and E. I. Duque, Phys. Rev. D **112**, 046022 (2025)
[54] M. Bojowald and G. M. Paily, Phys. Rev. D **86**, 104018 (2012)
[55] R. Tibrewala, Class. Quant. Grav. **31**, 055010 (2014)
[56] M. Bojowald, S. Brahma, and J. D. Reyes, Phys. Rev. D **92**, 045043 (2015)
[57] J.-P. Wu, M. Bojowald, and Y. Ma, Phys. Rev. D **98**, 106009 (2018)
[58] M. Bojowald, Phys. Rev. D **102**, 046006 (2020)
[59] R. Gambini, J. Olmedo, and J. Pullin, Phys. Rev. D **105**, 026017 (2022)
[60] M. Han and H. Liu, Phys. Rev. D **109**, 084033 (2024)
[61] K. Giesel, H. Liu, P. Singh, and S. A. Weigl, Phys. Rev. D **110**, 104016 (2024)
[62] M. Bojowald and E. I. Duque, Phys. Rev. D **109**, 084044 (2024)
[63] C. Zhang and Z. Cao, Phys. Rev. Lett. **135**, 261401 (2025)
[64] A. Ashtekar, T. Pawlowski, and P. Singh, Phys. Rev. Lett. **96**, 141301 (2006)
[65] R. Gambini and J. Pullin, Phys. Rev. Lett. **101**, 161301 (2008)
[66] R. Gambini, J. Olmedo, and J. Pullin, Class. Quant. Grav. **31**, 095009 (2014)
[67] A. Ashtekar, J. Olmedo, and P. Singh, Phys. Rev. Lett. **121**, 241301 (2018)
[68] C. Zhang, Y. Ma, S. Song, and X. Zhang, Phys. Rev. D **102**, 041502 (2020)
[69] V. Husain, J. G. Kelly, R. Santacruz, and E. Wilson-Ewing, Phys. Rev. Lett. **128**, 121301 (2022)
[70] A. Alonso-Bardaji, D. Brizuela, and R. Vera, Phys. Lett. B **829**, 137075 (2022)
[71] B. Elizaga Navascués, G. A. Mena Marugán, and A. M. Sánchez, Phys. Rev. D **108**, 106001 (2023)
[72] C. Zhang, Y. Ma, S. Song, and X. Zhang, Phys. Rev. D **105**, 024069 (2022)
[73] A. Alonso-Bardaji, D. Brizuela, and R. Vera, Phys. Rev. D **106**, 024035 (2022)
[74] C. Zhang, J. Lewandowski, Y. Ma, and J. Yang, Phys. Rev. D **111**, L081504 (2025)
[75] C. Zhang, J. Lewandowski, Y. Ma, and J. Yang, Phys. Rev. D **112**, 044054 (2025)
[76] M. Azreg-Aïnou, Phys. Rev. D **90**, 064041 (2014)
[77] Z. Ban, J. Chen, and J. Yang, Eur. Phys. J. C **85**, 878 (2025)
[78] B. Carter, Phys. Rev. **174**, 1559 (1968)
[79] Y. Shen, H.-Y. YuChih, and B. Chen, Phys. Rev. D **110**, 123010 (2024)

CTC Accepted